EX/P5-34

Microscopic Modification of Wall Surface by Glow Discharge Cleaning and its Impact on Vacuum Properties of LHD

M. Tokitani 1), M. Miyamoto 2), K. Tokunaga 3), T. Fujiwara 3), N. Yoshida 3), A. Komori 4), S. Masuzaki 4), N. Ashikawa 4), S. Inagaki 4), T. Kobuchi 4), M. Goto 4), J. Miyazawa 4), K. Nishimura 4), N. Noda 4), B.J. Peterson 4), A. Sagara 4) and LHD experimental group 4)

1) Interdisciplinary Graduate School of Engineering Science, Kyushu University, Kasuga, Fukuoka 816-8580, Japan
2) Department of Material Science, Shimane University, Matsue, Shimane, 690-8504, Japan
3) Research Institute for Applied Mechanics, Kyushu University, Kasuga, Fukuoka 816-8580, Japan
4) National Institute for Fusion Science, Oroshi, Toki, Gifu 509-5292, Japan

e-mail contact of main author: tokitani@riam.kyushu-u.ac.jp

Abstract. Glow discharge cleaning (GDC) is a widely used technique for wall conditioning in fusion experimental devices. Though the cleaning effects of GDC are essentially related to the microscopic modification of the wall surface, there are few reports about it. In the present study, samples of wall materials were exposed to GDC plasma of hydrogen, helium and neon in the Large Helical Device (LHD) by using the retractable material probe transfer system and examined microscopic modification by transmission electron microscopy (TEM) to understand the underlying mechanism of GDC. Based on the results of the material probe experiments, GDC of LHD was successfully improved. Reduction of the impurities in the LHD vacuum vessel was drastically improved by using Ne-GDC. In the case of Ne-GDC, the specimen surface was covered with very thick re-deposited layer of Fe and Cr. Due to its high sputtering efficiency and very shallow penetration, it is likely that neon atoms effectively sputtered surface contamination without remaining serious damage and themselves in the sub-surface region. Retained Ne can be successfully removed by the following short H-GDC.

1. Introduction

LHD is the largest heliotron-type plasma confinement device, and is equipped with superconducting magnetic coils. The first wall panels and the divertor plates of LHD are made of stainless steel (SUS316L) and isotropic graphite, respectively. The former is the major material in LHD, and the graphite area is only about 5 % of the total plasma facing area. The vacuum vessel temperature is limited up to 95 ˚C due to the cryogenic capability for superconducting magnetic coils. Wall conditioning is conducted by mild temperature (95 ˚C) baking, GDC and titanium or boron coating. Working gases for GDC are hydrogen (H), helium (He) and neon (Ne). Until the experimental campaign in 2002, He-GDC was most frequently conducted.

In large-size plasma confinement devices like LHD, GDC is applied as a convenient wall conditioning method. Helium is used for working gas in some cases. In case of the all stainless steel wall machine TJ-II stellarator, control of plasma density at medium and high power injection became difficult, because the helium implanted in the wall by He-GDC desorbed during main plasma discharge [1]. In case of LHD, in spite of pumping for 7 hours after He-GDC (for about 8 hours), the residual helium gas was still detected in the vacuum vessel [2]. Such prolonged desorption of helium gas made the ICRF heating condition unstable, and helium leak test difficult. It is well known that helium atoms implanted into metals are deeply trapped by lattice defects such as vacancies and bubbles formed by their own irradiation even if they do not have sufficient energy for knock-on damage [3].

In order to solve these problems, the behavior of implanted helium in metals (stainless steel) must be investigated from a viewpoint of material science. In the present work,

therefore, microscopic modification and retention properties in metals exposed to He-, H-, Ne-GDC in LHD were studied and its impact on vacuum properties of LHD is discussed by using several kinds of analytical techniques complementally. Based on the experimental results more efficient GDC method in LHD was proposed.

2. Experimental Procedures

To examine the surface modification and retention properties in metals due to the He-, H- and Ne-GDC, GDC exposure experiments carried out in the LHD. Pre-thinned vacuum annealed stainless steel (SUS316L) disks of 3mm in diameter and stainless steel (SUS316L) plates of 0.1 mm thick were used as specimens. All specimens were electrochemically polished. The specimens mounted on the retractable material probe system attached to the LHD, which is the same electric potential as the vacuum vessel, were placed on a position similar to the first wall surface through the 4.5 lower port (4.5L) as shown in Fig. 1. The GDC-plasma was sustained with two electrodes inserted into the vacuum vessel from the 4.5 upper port (4.5U) and the 10.5 upper port (10.5U). Discharge parameters of the GDCs were summarized in table 1. Total fluence was roughly estimated at 3.7×10^{22} He/m^2, 4.1×10^{22} H/m^2 and 3.2×10^{22} Ne/m^2 respectively, based on the total plasma-facing area of 780 m^2. The temperature of the probe head during the GDCs was measured by thermocouples at the positions just beneath the specimens. It stayed almost constant near room temperature.

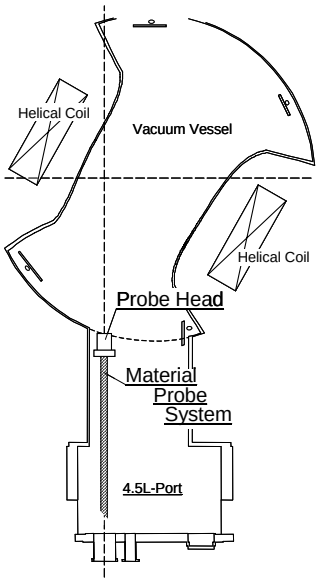

Fig. 1. Schematic view of the experimental position.

	Total discharge time	Voltage	Current
He-GDC	65h	200V	20A
H-GDC	71.5h	300V	20A
Ne-GDC	55h	200V	20A

Table 1. Discharge parameters of He, H and Ne-GDC.

After exposing to GDCs, microscopic damage, chemical composition and retention properties were examined by means of scanning electron microscopy (SEM), atomic force microscopy (AFM), transmission electron microscopy (TEM), energy dispersive spectroscopy (EDS) and thermal desorption spectroscopy (TDS).

Additional deuterium irradiation to the specimen pre-exposed to He-, H- and Ne-GDC was carried out in order to confirm the change of deuterium retention properties due to the GDCs. Samples of SUS316L (10x10x0.1 mm^3) exposed to GDCs were irradiated with 2 keV-D^+ at room temperature up to dose of 1×10^{22} D^+/m^2. And then the specimens were transferred into a TDS apparatus, where the thermally desorbed deuterium gas was measured with a high-resolution quadrupole mass spectrometer by heating up to 1400 K with a ramping rate of 1 K/s. This device makes it possible to distinguish the small difference in mass of helium (^{4}He: m=4.0026 amu) and deuterium gas (D_2: m=4.0282 amu) [4]. Desorption rate of deuterium was quantitatively calibrated by comparing with helium standard leak with specific relative ionization efficiency.

3. Results and Discussion

3.1. Microscopic modification and impurity depositions by GDCs

Fig. 2 shows TEM images of the pre-thinned SUS316L specimens exposed to He-, H- and Ne-GDC for 65h, 71.5h and 55h, respectively. The incident energy of these GDCs was at most about 200 eV, 300 eV and 200 eV, respectively. The temperature of the specimen holder during GDCs stayed almost constant near room temperature.

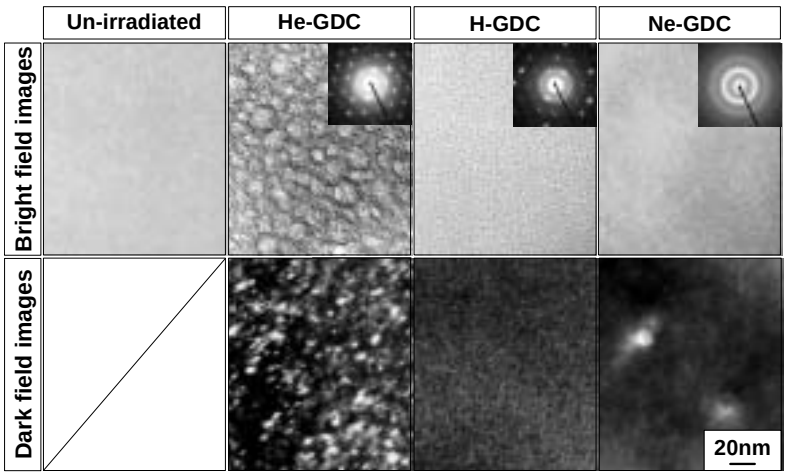

Fig. 2 TEM images after three GDCs, bright field images at large deviation parameter condition (upper series). White dot contrast in dark field images show dislocation loops (lower series).

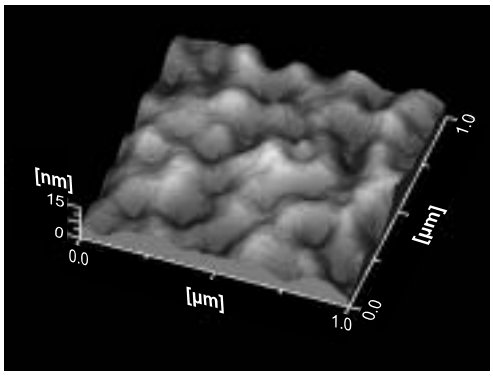

Fig. 3 Surface morphology of SUS316L after exposed to a He-GDC as observed by AFM.

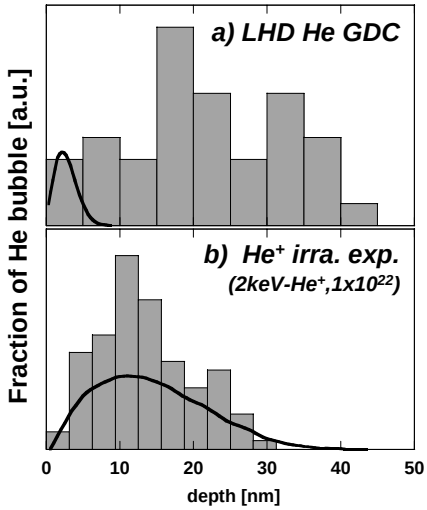

Fig. 4 (a)Depth distribution of helium bubbles in SUS316L exposed to He-GDC and (b) irradiated with 2keV-He^+ at room temperature to a fluence of 1×10^{22} He/m^2. Depth distribution of the helium calculated by TRIM91-code was also plotted together.

Special features of He-GDC were rather strong sputtering erosion and heavy damage at the subsurface region; formation of dense bubbles with size of 2-20 nm, dislocation loops and cracks connecting the bubbles. Such a heavy damage structure was formed in spite of low incident energy. It is known that despite of insufficient irradiation energy for knock-on damage, injected helium atoms aggregate by themselves without any pre-existing vacancies and form dense helium bubbles [3]. Surface morphology obtained by a high resolution micrograph of AFM observation of the SUS316L specimen after the exposure is shown in Fig. 3. The surface is covered with dimples of about 200-400 nm in size. They are probably formed by exfoliation of blisters. Such large dimples and large bubbles have not been observed for an irradiation with 2keV-He^+ at room temperature with comparable fluence [5]. In the case of helium ion irradiation experiment at

room temperature, very dense helium bubbles of about 1-2nm and dislocation loops were observed. Formation of dense helium bubbles, exfoliation of blisters and cracks lead to the increase of the effective surface area of the materials. It is expected that the increase in surface area causes adsorption of impurities gas existing in the vacuum vessel.

The depth distribution of helium bubbles formed in SUS316L exposed He-GDC is plotted in Fig. 4 together with the depth distribution of the helium calculated by TRIM91-code for 200eV-He^+. The data for irradiation experiment with 2keV-He^+ at room temperature is also plotted in the Fig. 4 for comparison. In case of He-GDC, the helium bubble was distributed deeper than the injected range. In contrast, in case of helium ion irradiation, distribution of a helium bubble agrees well with the injected range. This difference seems to be the result of the concentration of vacancies formed by knock-on process. In the case of 2keV-He^+, almost all the injected helium is trapped by the radiation induced vacancies which are formed in the helium injected range. In He-GDC case, since radiation induced vacancies are not formed, injected helium atoms can diffuse far deeper than the injected range, until it form their stable clusters. It is likely that some part of helium trapped in the heavily damaged region may release gradually through the nano-cracks connecting the bubbles and the surface. The prolonged helium release currently observed at LHD after helium-GDC can be explained from this mechanism [2]. As shown in Fig. 5, desorption of helium is also affected by hydrogen discharge; in spite of no helium supply from outside, helium content in plasma increased during hydrogen discharges performed just after He-GDC.

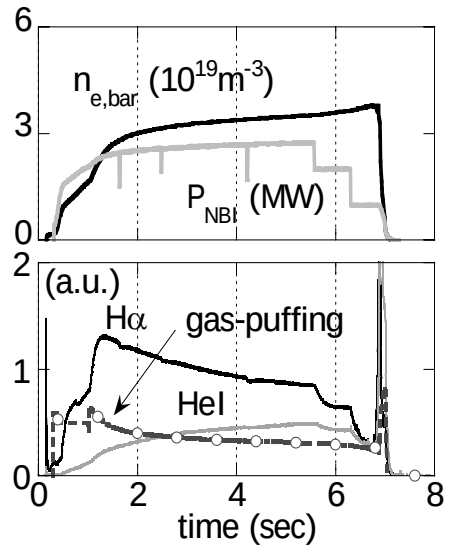

Fig 5. A typical discharge after He-GDC with hydrogen gas-puffing. (#26500)

On the other hand, accumulation of defects such as bubbles was not observed in the specimens exposed to H-GDC and Ne-GDC (see Fig. 1). After exposure, impurity deposits were also identified on the specimens. Fig. 6 shows the electron diffraction pattern and the dark field image of deposition layer formed on SUS316L specimens exposed to GDCs. White contrasts show individual crystal grains of deposits. Especially, in case of Ne-GDC, the contrast of diffraction pattern is the clearest. This means that the specimen surface was covered with thick deposition layer. Due to its high sputtering efficiency, about ten times higher than that of helium, and very shallow penetration, it is likely that neon atoms effectively sputtered surface contamination without remaining serious damage and themselves in the sub-surface region. The element of deposition layers detected by EDS is mainly Fe and Cr, which

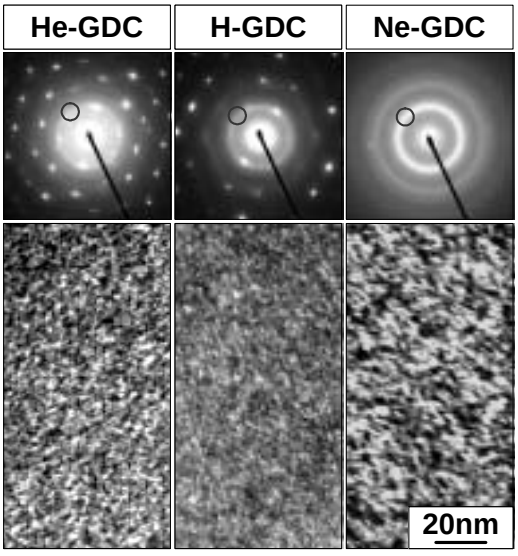

Fig. 6 Electron diffraction pattern and the dark field image of deposition layer formed on SUS316L exposed to GDCs. White dots show individual crystal grains of deposits.

were probably sputtered from the first wall of LHD (SUS316L). In the case of H-GDC, because the energy is insufficient for knock-on damage, the irradiation damage was not formed. Furthermore, due to its low sputtering efficiency, re-deposition of impurities is also very little (see Fig. 6).

3.2. Retention of deuterium after GDCs

Fig. 7 shows TDS of deuterium injected in the SUS316L specimens pre-exposed to He-(65h), H-(71.5h) and Ne-GDC(55h). Deuterium irradiation was performed subsequently at room temperature with 2keV-D^+ up to dose of $1x10^{22}$ D^+/m^2 is plotted in Fig. 7 (a), and without pre-exposes case (fresh specimen) was also shown in Fig. 7 (b). In case of the fresh one, thermal desorption spectra of deuterium is broad, and desorption is continued from 300K to 500 K, but a sharp peak has appeared in the samples exposed to GDCs. The total retention is shown in Fig. 8. The fresh specimen has the highest deuterium retention. Namely, it was shown that the total retention of deuterium becomes lower by performing GDCs. Its mechanism is not understood well at the present, but it may have influenced that the oxide thin film of the surface was removed by performing GDCs. It was reported that an oxide film at the surface affects the retention and the diffusion of deuterium [6,7].

He-GDC showed highest deuterium retention and Ne-GDC showed lowest deuterium retention among the three GDCs. In the case of He-DGC, most of the injected deuterium ions (2keV) are stopped in the heavily damaged layer of about 40 nm (see Fig. 4), because their projected range is about 20 nm. Therefore, it is considered that possible trapping sites for deuterium injected in the sample exposed to He-GDC is helium bubbles and strong stress field around them. It was reported that the stress fields around the highly pressurized helium bubbles in tungsten act the effective trapping sites of deuterium [8]. In contrast with He-GDC, Ne-GDC showed lowest retention of deuterium. Sufficient amount of trap sites for injected deuterium does not exist, because radiation induced defects are scarcely formed.

In case of H-GDC, desorption temperature shifts to lower side comparing with He-GDC, Ne-GDC and even the fresh specimen case. Most of the retained deuterium detraps up to 95 ˚C. We can say that this is one of a surface cleaning effect of H-GDC. This result indicates that it is possible in LHD to remove hydrogen effectively from the surface treated by H-GDC by the usual backing at 95 ˚C.

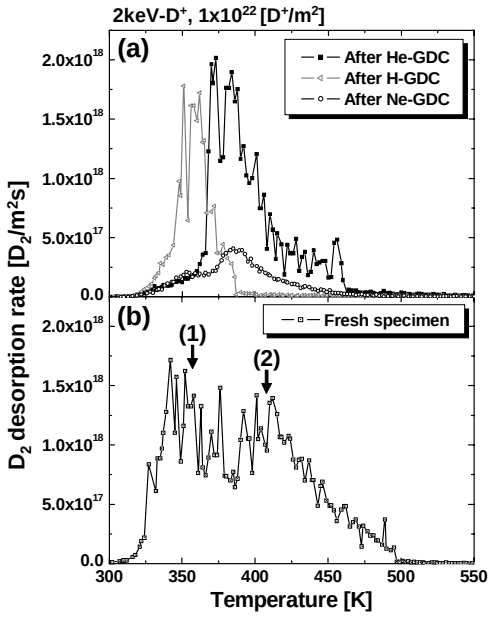

Fig. 7 Thermal desorption spectra of deuterium (a) with pre-exposes of GDCs and (b) without pre-exposes (Fresh specimen).

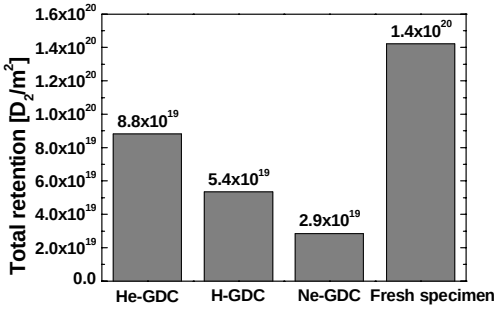

Fig. 8 Total desorption of deuterium in SUS316L, After GDCs and fresh specimen.

3.3. Improvement of GDC

Based on the results of the material probe experiments mentioned above, improved GDC technique was proposed; a two-step GDC method, combination of a Ne-GDC for efficient sputtering of surface contamination and a successive short H-GDC to desorbs Ne retained during the first Ne-GDC. At the beginning of the experimental campaign in 2003, this two-step method was conducted to shorten the wall conditioning process and suppress the undesired desorption of the working gas of the GDC. Fig. 9 shows the reduction of partial pressure of M=28 (CO) measured by quadrupole mass spectrometer during He-GDC and Ne-GDC. The decay time for Ne-GDC is much shorter and the achieved partial pressure was one order lower than those for He-GDC. These results are due to the high sputtering yield and very shallow penetration of Ne-GDC. After the Ne-GDC phase, H-GDC was conducted to remove implanted Ne in the first wall panels and the divertor plates. The partial pressure of Ne was reduced to the initial level after about 12 hours of H-GDC.

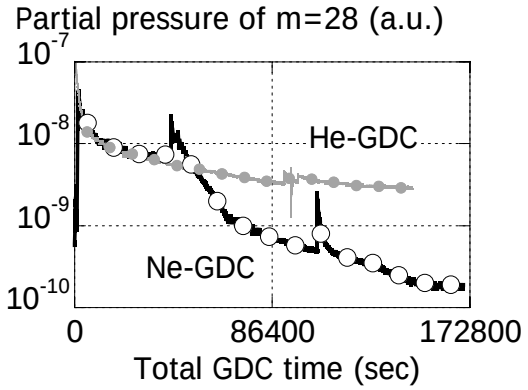

Fig. 9 Partial pressure of m=28 versus total GDC time.

4. Summary

The material probe experiments were carried out by exposing the SUS316L specimens to three different types of GDCs in LHD. Special features of He-GDC were rather strong sputtering erosion and heavy damage at the subsurface region; formation of dense bubbles with size of 2-20 nm, dislocation loops and cracks connecting the bubbles. The surface is covered with large dimples which seem to be formed by exfoliation of blisters. Such a heavily damaged structure leads to an increase of the effective surface area of a LHD vacuum vessel wall. It was suggested that He-GDC has a disadvantage as a wall conditioning. On the other hand, in cases of H-GDC and Ne-GDC, irradiation damages were not observed. However, thick deposition layers were observed on the sample after Ne-GDC.

The influence of the GDCs on the deuterium retention was also examined. The sample exposed to He-GDC showed highest deuterium retention while Ne-GDC showed lowest. In case of H-GDC, most of deuterium desorbs up to 95˚C.

It is considered that Ne-GDC and H-GDC is more suitable for GDC. At the beginning of the experimental campaign in 2003, Ne-GDC was conducted for efficient wall conditioning, due to its high sputtering efficiency and very shallow penetration. After the Ne-GDC phase, short H-GDC was conducted to remove implanted Ne.

It should be emphasized that understanding of characteristic feature of the microscopic processes of damage and surface modification for each GDC with different working gas was very effective for improvement of wall conditioning process of LHD.

Reference

[1] D. Tafalla, F.L. Tabares, J. Nucl. Mater. 290-293 (2001) 1195-1198
[2] H. Suzuki et al., J. Nucl. Mater. 313-316 (2003) 297-301
[3] H. Iwakiri et al., J. Nucl. Mater. 283-287 (2000) 1134-113
[4] S. Hiroki et al., J. Nucl. Mater. 224 (1995) 293-298
[5] M. Tokitani et al., J. Nucl. Mater. 329-333 (2004) 761-765
[6] Y. Ishikawa et al., Vacuum, 47, 6-8, 701-704 (1996)
[7] T. Hino et al., J. Nucl. Mater. 329-333 (2004) 673-677
[8] H. Iwakiri et al., J. Nucl. Mater. 307-311 (2002) 135-138